JOURNAL OF THE MECHANICAL BEHAVIOR OF BIOMEDICAL MATERIALS 58 (2016) 139–148

Available online at www.sciencedirect.com

ScienceDirect

www.elsevier.com/locate/jmbbm

Research Paper

A simple, effective and clinically applicable method to compute abdominal aortic aneurysm wall stress

Grand Roman Joldes[a,1], Karol Miller[a,*,1], Adam Wittek[a], Barry Doyle[a,b]

[a]Vascular Engineering, Intelligent Systems for Medicine Laboratory, The University of Western Australia, 35 Stirling Highway, Perth, WA 6009, Australia
[b]Centre for Cardiovascular Science, The University of Edinburgh, UK

ARTICLE INFO

Article history:
Received 29 April 2015
Received in revised form
22 July 2015
Accepted 27 July 2015
Available online 5 August 2015

Keywords:
Abdominal aortic aneurysm
Patient specific modelling
Finite element method
Inverse problems

ABSTRACT

Abdominal aortic aneurysm (AAA) is a permanent and irreversible dilation of the lower region of the aorta. It is a symptomless condition that if left untreated can expand to the point of rupture. Mechanically-speaking, rupture of an artery occurs when the local wall stress exceeds the local wall strength. It is therefore desirable to be able to non-invasively estimate the AAA wall stress for a given patient, quickly and reliably.

In this paper we present an entirely new approach to computing the wall tension (i.e. the stress resultant equal to the integral of the stresses tangent to the wall over the wall thickness) within an AAA that relies on trivial linear elastic finite element computations, which can be performed instantaneously in the clinical environment on the simplest computing hardware. As an input to our calculations we only use information readily available in the clinic: the shape of the aneurysm in-vivo, as seen on a computed tomography (CT) scan, and blood pressure. We demonstrate that tension fields computed with the proposed approach agree well with those obtained using very sophisticated, state-of-the-art non-linear inverse procedures. Using magnetic resonance (MR) images of the same patient, we can approximately measure the local wall thickness and calculate the local wall stress. What is truly exciting about this simple approach is that one does not need any information on material parameters; this supports the development and use of patient-specific modelling (PSM), where uncertainty in material data is recognised as a key limitation.

The methods demonstrated in this paper are applicable to other areas of biomechanics where the loads and loaded geometry of the system are known.

1. Introduction

Abdominal aortic aneurysm (AAA) is a permanent and irreversible dilation of the lower region of the aorta. It is typically a symptomless condition that if left untreated, can expand to the point of rupture. There are many limitations to the current clinical definition of 'high-risk' and many researchers believe that patient-specific modelling (PSM) could have major clinical

*Corresponding author. Tel.: +61 8 6488 8545.
E-mail address: karol.miller@uwa.edu.au (K. Miller).
[1]These authors contributed equally to this work.

http://dx.doi.org/10.1016/j.jmbbm.2015.07.029

potential (McGloughlin and Doyle, 2010; Vande Geest et al., 2006b; Gasser et al., 2010; Gasser et al., 2014).

Mechanically-speaking, rupture of an artery occurs when the local wall stress exceeds the local wall strength. Whilst Vande Geest et al. proposed a useful statistical model for wall strength[2] (Vande Geest et al., 2006a) which has subsequently been used in many rupture assessment studies (Maier et al., 2010; Gasser et al., 2010, 2014; Erhart et al., 2015; Hyhlik-Durr et al., 2011; Doyle et al., 2013); it is important we remember that we have absolutely no *a priori* information of a person's material data.

With the advances in medical imaging technology and medical image analysis software, it became possible to create patient-specific reconstructions of the AAA, which were then used for computer simulations that have steadily increased in complexity (Raghavan et al., 2000; Doyle et al., 2007; Gasser et al., 2010; Li et al., 2010). Major research efforts have been preoccupied with material models and simulations so comprehensive that they require inaccessible (in a typical clinic) computer power and specialist knowledge to implement. Many of the published results have been obtained by directly applying pressure loads to the already loaded configuration and therefore may not be true representations of the in vivo situation.

In this paper an entirely new, very simple approach is proposed and validated. What is truly exciting about this simple approach is that one does not need any information on material parameters; this supports the development and use of PSM, where uncertainty in material data is recognised as a key limitation.

The paper is organised as follows. In Section 2, we discuss the key differences between the data available in an engineering research laboratory conducting experiments, and those available in a typical clinic. In Section 3 we then use a phantom AAA geometry (Doyle et al., 2010) to demonstrate the equivalence of stress fields computed using (i) direct non-linear finite element procedure taking an undeformed configuration, exact material properties, and pressure load as inputs and (ii) inverse non-linear procedure (Joldes et al., 2015; Miller and Lu, 2013; Lu et al., 2007b) taking the deformed configuration and pressure load as inputs (note that knowledge of material parameters is not needed). We then propose a simple linear elastic calculation providing results equivalent to those of a sophisticated inverse procedure. In Section 4 we demonstrate the applicability of the proposed method to clinical cases and highlight the importance of accurate measurement of the wall thickness. Finally we provide conclusions, discussion and suggestions for future work in Section 5.

2. Engineering laboratory vs. a typical clinic

A typical engineering laboratory at a university or hospital is able to readily conduct the following experiment (Doyle et al., 2010). Firstly, construct a “rubber aneurysm” (Fig. 1) from a material (typically a specially mixed silicone with precisely known material properties (Doyle et al., 2009)) with the geometry provided by a reconstruction of a computed tomography (CT) scan of a real clinical case (Doyle et al., 2008). As with any experimental phantom, it is difficult to ensure exact uniformity of the wall thickness, therefore, by imaging the phantom with CT; the precise wall thickness can be obtained. Then the “rubber aneurysm” can be pressure-loaded and its deformed configuration measured precisely, together with the surface strain field (e.g. by stereoscopic techniques (Meyer et al., 2011) or the photoelastic method (Doyle et al., 2012)). The load can be increased until the “rubber aneurysm” ruptures and the rupture site can then be located. We can then compare this position to the high stress regions computed using a standard direct non-linear finite element procedure (available in a plethora of commercial FEM packages) taking as inputs the known undeformed configuration (including thickness), precisely known parameters of the constitutive material model and the applied pressure load.

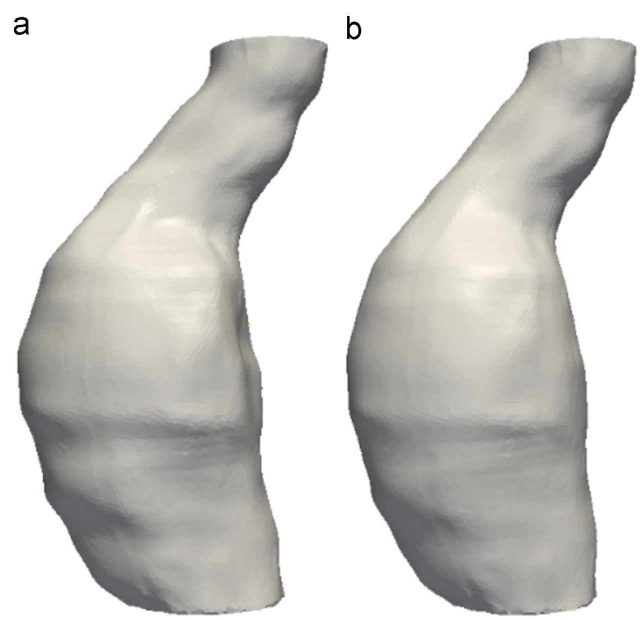

Fig. 1 – (a) Undeformed and (b) deformed configuration of a “rubber aneurysm” (Doyle et al., 2012).

In contrast, the situation in a typical clinic is very different: the overall geometry of a loaded aneurysm can be seen on a CT and then extracted like shown in Fig. 2 (e.g. using medical image analysis software such as TeraRecon, Mimics or 3D Slicer) and the pressure load can be measured at the time of imaging. It is however imperative to note that none of the following is known: unloaded configuration, constitutive material model and its parameters for a given patient, and the wall thickness. Recent efforts have reported a method of obtaining wall thickness from typical CT (Shang et al., 2015) however this technique is yet to be widely adopted and tested.

Therefore, to bring computational biomechanics into the clinic, we need to devise modelling and simulation methods which will use only (very limited) data available in the clinic.

3. Computing wall stress in a “rubber aneurysm”

Doyle et al. (2010) provided wealth of data useful for validating approaches to computing AAA wall stress, as described in

[2]The issue of wall strength is an entirely different matter and not addressed in this work.

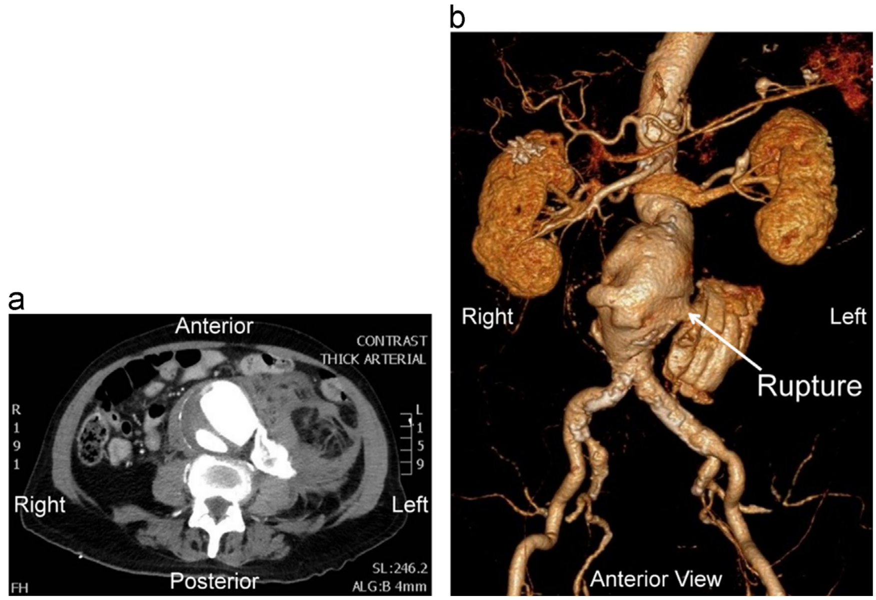

Fig. 2 – Real AAA case. Only deformed geometry and pressure load can be reasonably easily extracted. (a) Axial CT scan showing rupture and (b) reconstructed geometry (Doyle et al., 2014).

Section 2. In Fig. 3a we present the stress field computed using a direct, non-linear procedure available in ABAQUS, with 120 mmHg load applied to the inner surface of the undeformed configuration (Fig. 1a). The constitutive law for the material used in the phantom construction was a 1st order Ogden hyperelastic model with parameters $\mu=1.6525$ MPa and $\alpha=0.6988$ MPa (Doyle et al., 2009). The finite element mesh used consists of approx. 200k hybrid elements and 50k nodes, with the nodes on the upper and lower ends of the AAA mesh fixed. Fig. 3b contains the same stress distribution obtained using a non-linear inverse procedure, starting from the deformed configuration (Fig. 1b), the same 120 mmHg load, the same material properties and using the same finite element mesh.

We note the fact that the stress computed using the specified procedures is Cauchy stress, defined as a physical quantity that expresses the internal forces that neighbouring particles of a continuous material exert on each other, expressed with respect to the deformed configuration. For a general 3D problem, the Cauchy stress is expressed as a symmetric tensor having six independent components; therefore, the von Misses stress is used in the following figures to characterise the complex stress state at any point of the material.

A number of equivalent inverse procedures can be used to solve the inverse problem. The method we used is an iterative approach taken from Riveros et al. (2013). The procedure consists of a series of direct computations, with the initial geometry being corrected using the difference between the computed deformed geometry and the desired (known) deformed geometry. The computations are repeated until the size of the correction to be applied to the initial geometry is smaller than a selected threshold. This is not efficient but can be performed using commercial code such as ABAQUS. More efficient methods exist (Lu et al., 2007b; Gasser et al., 2010; Joldes et al., 2015) but they require specialised software.

As can be seen in Fig. 3, the computed stress fields are for practical purposes the same; the negligible differences are due to the termination criterion used to stop the iterative inverse procedure, which requires that the difference between the nodal positions in the deformed configurations (the input one and the one obtained from the computed undeformed configuration) is less than 0.001 mm.

The problem of solving a blood pressure loaded AAA resembles that of a pressure vessel loaded by internal pressure, frequently encountered in mechanical design handbooks. It is known that such pressure vessels are statically determinate even when the walls are not "thin" and therefore the stress in the wall depends only on its geometry and the applied internal pressure, and does not depend on the material properties of the wall (see e.g. Budynas et al. (2011)). It is therefore expected, even before conducting a detailed analysis, that the stress field should be only very weakly dependent on the mechanical properties of the tissue (Miller and Lu, 2013). This is very important because for a "rubber aneurysm" we know these properties precisely, while for a given patient, these properties are impossible to determine.

To demonstrate this, in Fig. 4 we present the stress fields computed using the non-linear inverse procedure for vastly different mechanical properties of the wall material. In the first three cases we used a linear elastic material with Young's modulus varying between 1.5 MPa and 10 MPa and Poisson's Ratio of 0.49 (almost incompressible). In the last case we used the anisotropic Holzapfel–Gasser–Ogden material model (Gasser et al., 2006) available in ABAQUS, with material parameters from Lu et al. (2007a): $C_{10}=0.3$ MPa, $D=0$, $k_1=2$ MPa, $k_2=1.25$, $k=0$, $N=2$, $\gamma=\pm 36.25^{\circ}$ (2 families of fibres oriented at $\pm 36.25^{\circ}$ in the global xOz plane). Normally, the material fibres should be oriented in local normal–axial–tangential coordinate systems for each element; defining such a local coordinate system for each element is not trivial and defies the purpose of this paper. Configuring the material fibres orientations in the global coordinate system is a convenient way to define an anisotropic material model with spatial inhomogeneity. The chosen material stiffens in the fibre plane for larger deformation since the fibre stiffness is modelled by an exponential function, whereas the stiffness normal to the fibre plane is modelled by a tensor linear (Neo-Hookean) model. Therefore the fibres will increase the material strength in the areas where the AAA surface is parallel to the global xOz plane and will have very limited effect in the areas where the AAA surface is perpendicular to the global xOz plane. This can be clearly noticed in Fig. 5c, where the ratio of maximum displacement in the xOz plane to maximum displacement in the yOz plane is much larger than in the case of homogenous materials (Fig. 5a and b).

As shown on Fig. 4, the computed stress fields are for practical purposes equivalent, thus demonstrating that when

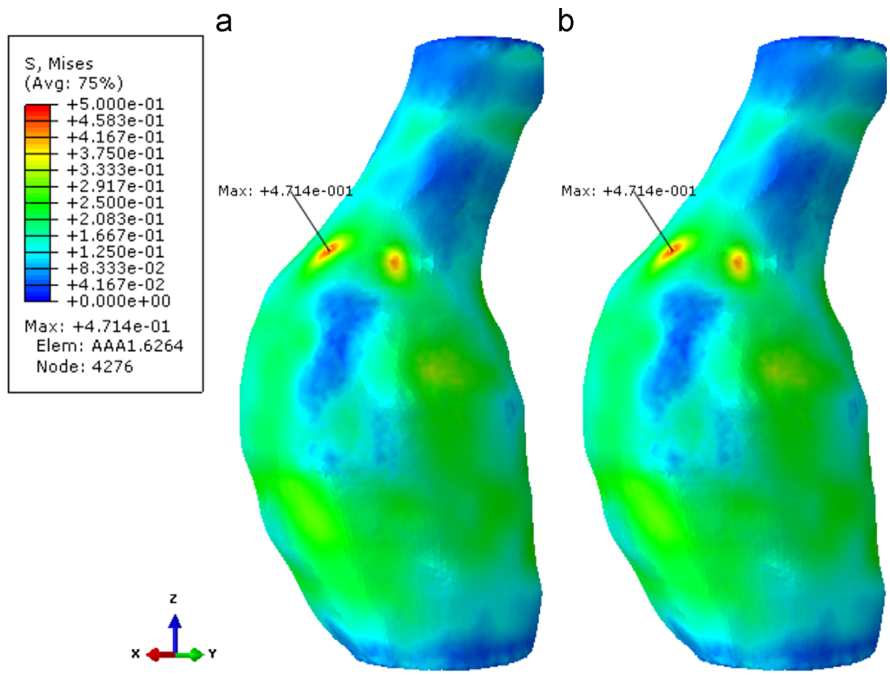

Fig. 3 – Rubber aneurysm analysis: von Mises stress mapped on the deformed geometry. (a) Direct solution, max stress 0.47141 MPa; (b) inverse solution, max stress 0.47144 MPa. The finite element mesh used consists of approx. 200 k hybrid elements and 50 k nodes.

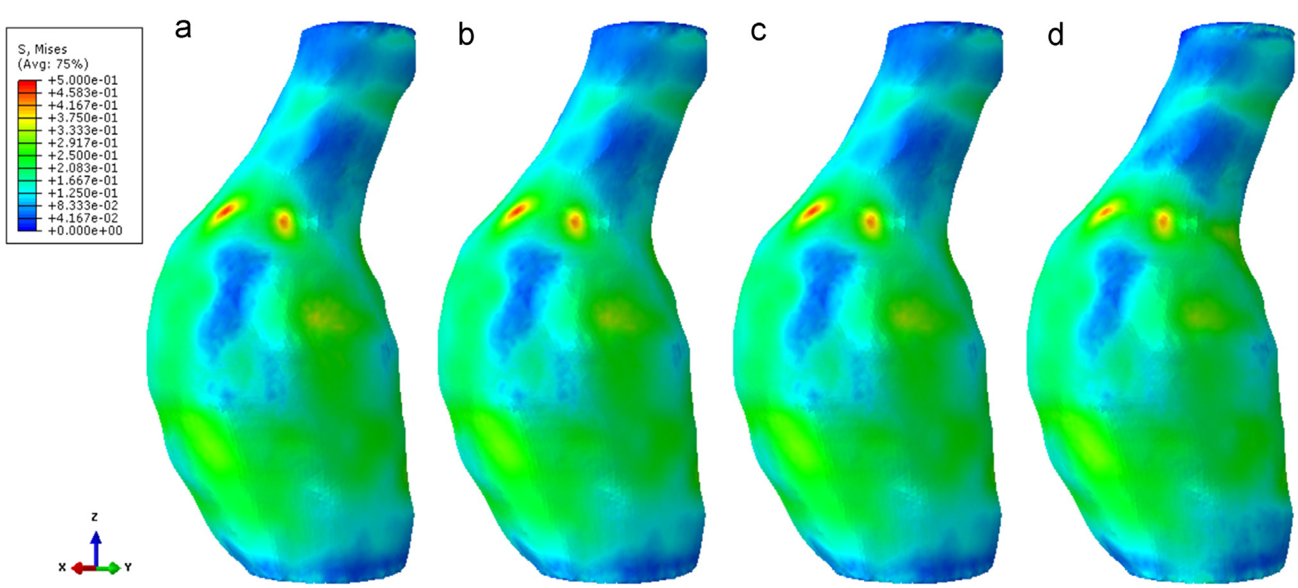

Fig. 4 – Stress fields computed using non-linear inverse procedure with vastly different mechanical properties of wall material. Linear elastic material with (a) $E=1.5$ MPa; (b) $E=5$ MPa; (c) $E=10$ MPa; in all cases the max. von Mises stress is $\sim$0.47 MPa. (d) An inhomogeneous, anisotropic material; max. von Mises stress is $\sim$0.44 MPa.

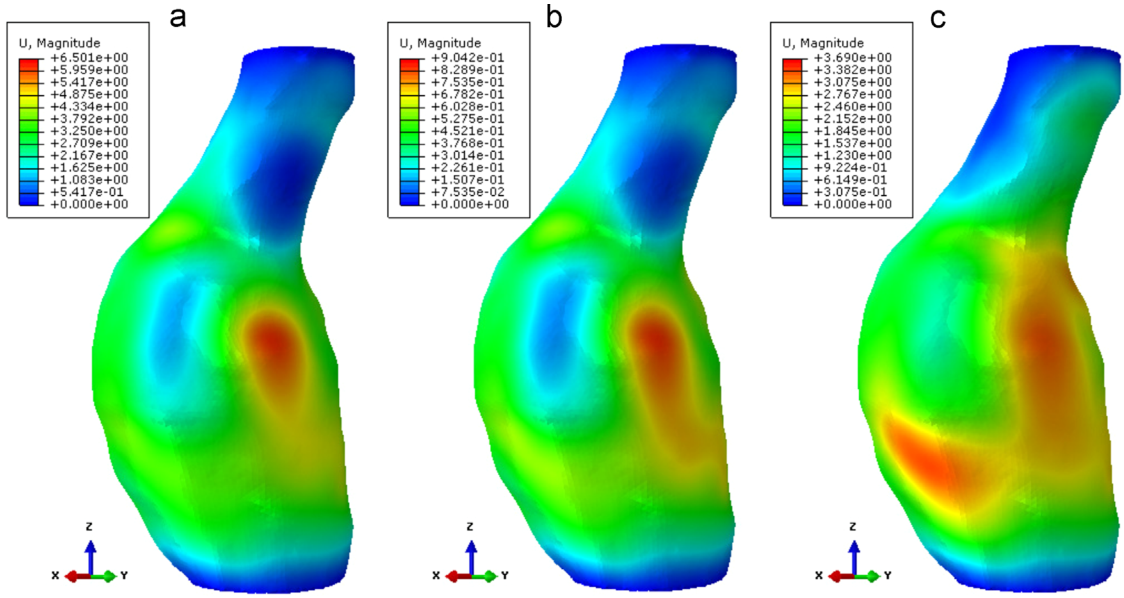

Fig. 5 – Displacement fields, in mm, computed using non-linear inverse procedure with vastly different mechanical properties of wall material: (a) Linear elastic material, $E=1.5$ MPa; (b) Linear elastic material, $E=10$ MPa; (c) An inhomogeneous, anisotropic material. Note the very different displacement scales used in each image.

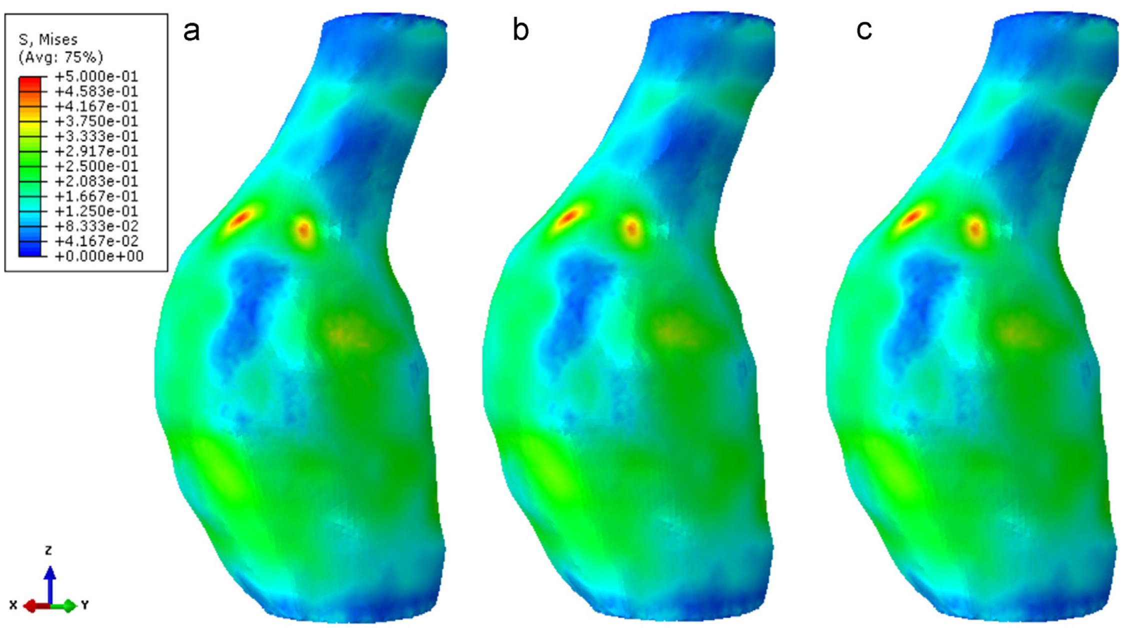

Fig. 6 – Stress fields for our "rubber aneurysm" (Fig. 1) computed using (a) a complicated nonlinear inverse procedure (see also Fig. 3), $E=1.5$ MPa, max. von Mises stress $=0.478$ MPa; (b) Very stiff material $E=1000$ MPa, max. von Mises stress $=0.475$ MPa; (c) Simple linear elastic computation, $E=1$ MPa, max von Mises stress $=0.475$ MPa.

using correctly an inverse solution procedure, one is able to estimate stresses well without knowing patient-specific properties of tissues. Of course this is not the first time this has been noticed; see e.g. Miller and Lu (2013) and Lu et al. (2007b).

One could argue that the material models may be very similar and the strains very small, and therefore the resulting stresses are similar. To counteract such arguments, we present the displacements computed for the different material models in Fig. 5. The results demonstrate that even if the stress values and distribution are very similar, the material model has a strong influence on the value and distribution of displacements (the undeformed configurations are very different when the material model changes).

The reason why the inverse approach works so well even in the absence of the knowledge of the constitutive properties of the continuum, is the fact that the structure under consideration is (approximately) statically determinate and

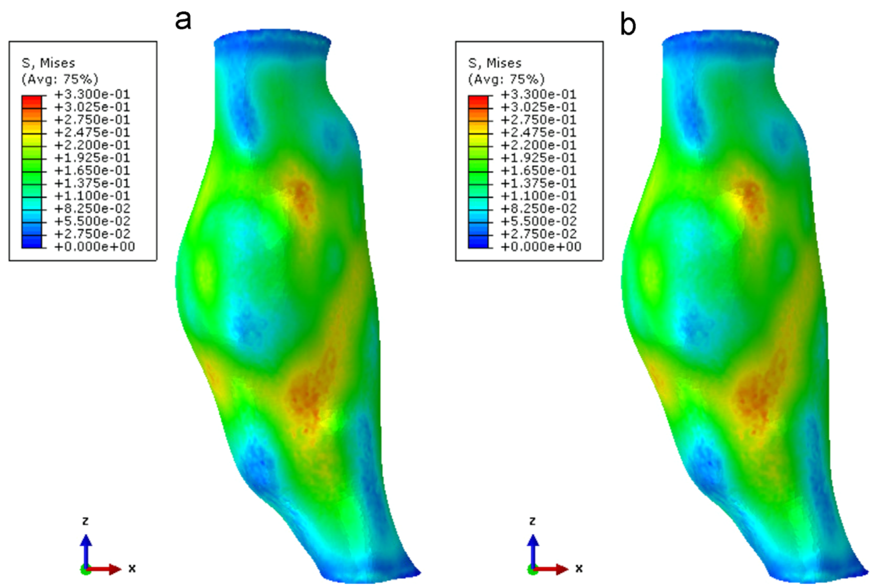

Fig. 7 – Analysis of a real AAA under the assumption of constant wall thickness. Comparison of stress fields computed (a) a nonlinear inverse procedure; $E=5$ MPa, max. von Mises stress = 0.326 MPa and (b) Linear elastic computation; max. von Mises stress = 0.325 MPa. The finite element mesh consists of approx. 400k hybrid elements and 83k nodes.

therefore statics is sufficient to compute internal forces (i.e. stress field) that balance the external loads (i.e. pressure). This realisation prompts the following conclusion: if we set-up the simulation in such a way that the deformed geometry remains unchanged under load, we should obtain the stress field that balances the external pressure. One simple way to achieve this is to specify a very stiff material, so that the strains under realistic pressure loads are infinitesimal (the geometry does not change), and conduct a linear stress analysis. Given the fact that in a linear finite element analysis the geometric configuration is assumed constant, the use of a stiff material is not even necessary as long as the load is applied in a single load step. In Fig. 6, we compare the stress field of our “rubber aneurysm” (Fig. 1) computed using an inverse nonlinear procedure and that computed using a linear analysis.

As expected, for practical purposes the stress fields are the same. This result demonstrates that the stress distribution in a pressure-loaded phantom aneurysm can be computed using simple linear elastic finite element procedure.

4. Tension and stress in real aneurysms

4.1. *Case without thrombus*

The results and conclusions of Section 3 can be directly translated to real cases.

In Fig. 7, we demonstrate stress fields for one of the clinical cases recruited to the MA^{3}RS Trial (McBride et al., 2015) using a nonlinear inverse solution procedure and a simple linear elastic one. In this example we assume a constant wall thickness of 2 mm. This case had only a minimal amount of thrombus and it was not included in the model.

As expected, the stress fields are for practical purposes the same. It is very important to note that the stress field given in Fig. 7b can be obtained without any difficulty in a clinic. No assumption about mechanical properties is made and the computation is sufficiently simple to be performed on easily accessible and unobtrusive computing hardware.

In order to explain the influence of wall thickness on the stress computation, we consider the AAA as a statically determined thin wall structure (having constant stress over the wall thickness). Therefore, we can define the wall tension as the product between the wall stress and the wall thickness. Under this assumption, any variations in the wall thickness will not affect the computed wall tension (which balances the applied pressure), but will have a very important effect on the stress. Fig. 8 explicitly demonstrates this on our “rubber aneurysm” (Fig. 1), where the stress and tension fields are shown together with the wall thickness. Even if the thin wall assumption does not completely hold for an AAA, it is still expected that wall thickness will have a significant influence on the computed stress field.

Under the common assumption of a constant wall thickness, the tension and stress fields are essentially the same (to a factor). However, as shown in Fig. 8, for variable wall thickness the stress field looks very different to a tension field. Therefore, the measurement of the wall thickness in the clinic appears to be an essential ingredient necessary for a reliable estimation of the stress field. This measurement can perhaps be performed by combining data from CT and Magnetic Resonance Imaging (MRI), see Fig. 9, although this presents itself as a significant challenge given the typical resolution of clinical images and the fact that MRI is not routine in AAA management.

Nevertheless, using a combination of MRI and CT we created a variable thickness wall by approximating the thickness, based on information from registered CT and MRI images, at several points on the AAA surface and then interpolating those values (Fig. 10c). The MRI to CT registration was performed using the SegmentationAidedRegistration module (Gao et al., 2012) available in 3D Slicer. Using this approach we have been able to compare the estimates of wall stress and tension in a real clinical case (see Fig. 10). Tension and stress fields are qualitatively different, highlighting the need for measuring wall thickness in the clinic.

4.2. *Case with thrombus*

In this section we consider a case with thrombus. This particular AAA was from a 69 year old male, with a maximum anterior–posterior diameter of 107 mm, selected from the IMPROVE Trial (IMROVE trial investigators, 2014). The AAA was reconstructed from the CT data and we found that 79% of the total AAA volume (806 cm^3) was occupied with intraluminal thrombus (ILT). The ILT varied in thickness from 1 to

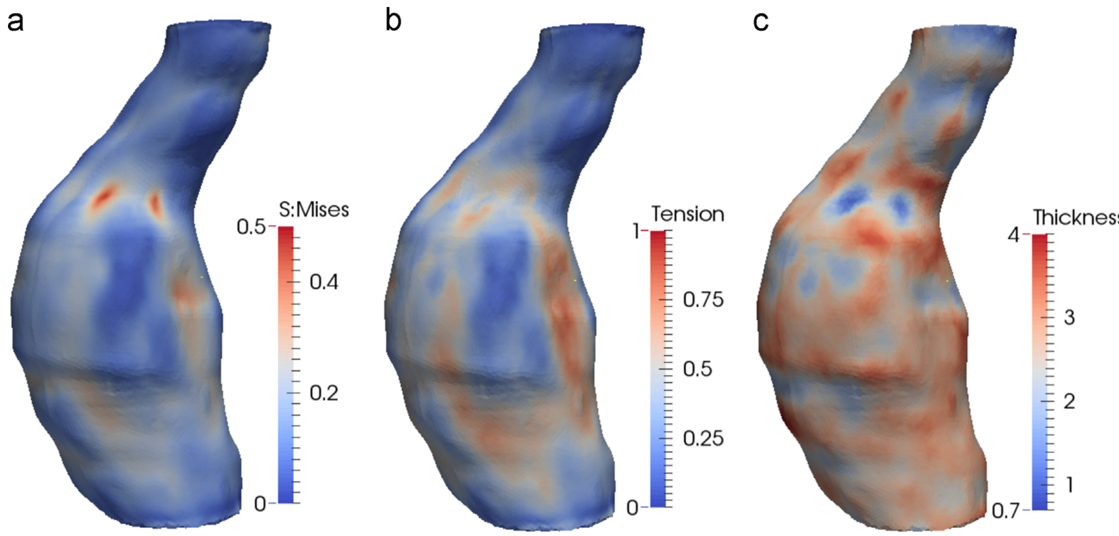

Fig. 8 – Analysis of our "rubber aneurysm". (a) Stress field. (b) Tension field – computed as the product between the stress and wall thickness, under the assumptions of uniform stress distribution over thickness. (c) Wall thickness.

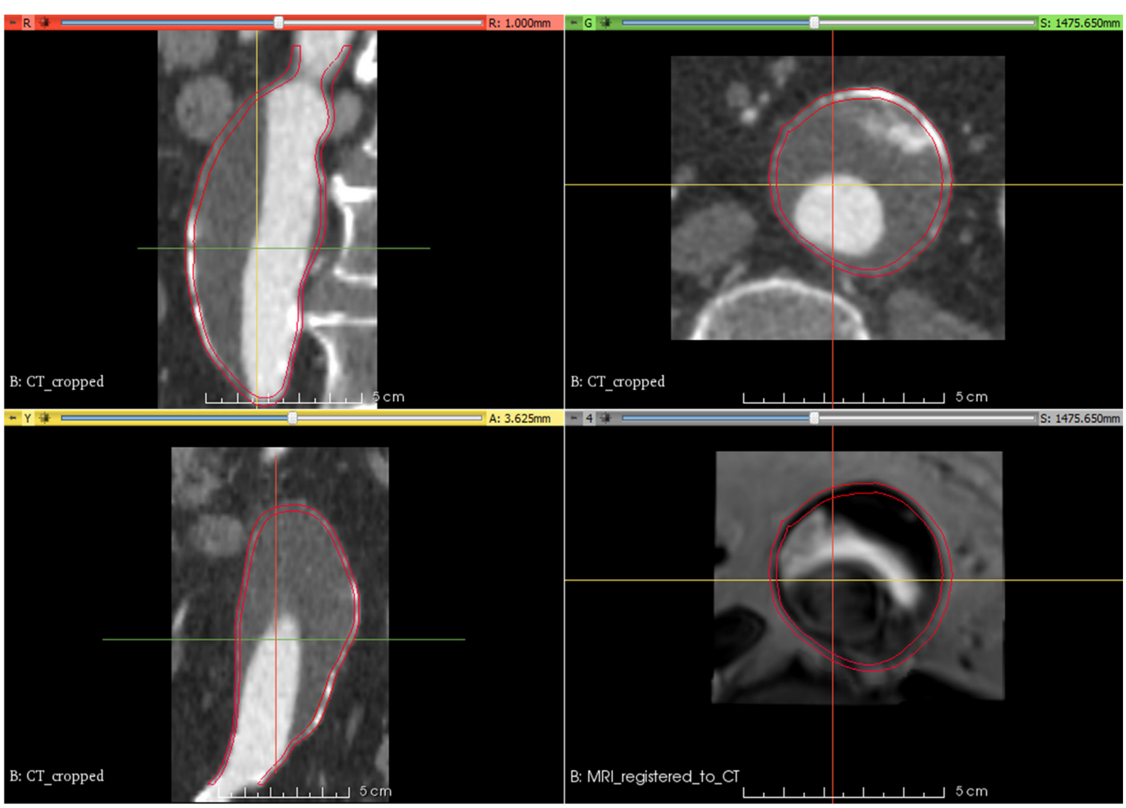

Fig. 9 – Combined CT-MRI datasets may help to capture wall thickness.

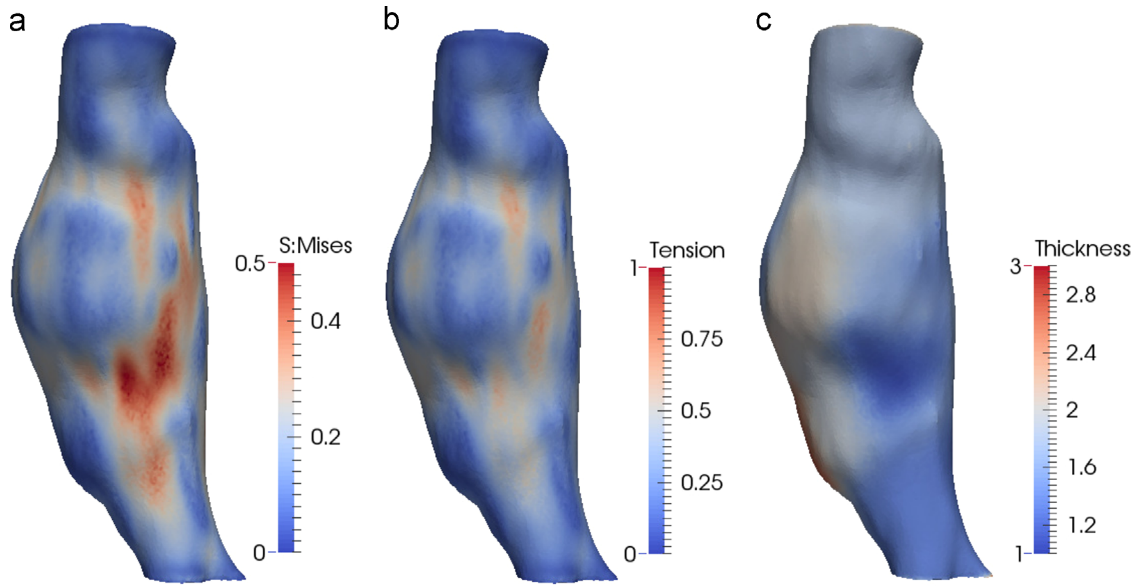

Fig. 10 – Stress (a), tension (b) and wall thickness (c) for a real aneurysm. While tension balances the internal pressure, the resulting stress field is qualitatively different, with much higher stresses in the areas of smaller thickness. This highlights the need for a measurement of the wall thickness in the clinic.

70 mm, and here we assume a uniform wall thickness of 1.5 mm. In addition to the AAA, the patient also had an aneurysmal disease in the common and internal iliac arteries. The results of this analysis are shown in Fig. 11 and it can be seen that the computed stress distributions are, for practical purposes, the same (less than 1% difference in computed maximum von Mises stress). We point out that when the material stiffness is scaled in order to prevent changes in the geometry, the ratio of stiffness between the different materials in the model has to be kept constant (the stiffness of all materials must be scaled by the same factor), as otherwise the distribution of stress between the different material layers would change. Therefore, for cases with ILT, a constitutive assumption about the ratio of wall and thrombus stiffness must be made, but fortunately the range of applicable values is reasonably well documented in the literature (O'Leary et al., 2014a, 2014b; Tong et al., 2011; Vande Geest et al., 2006c; Di Martino et al., 2006).

5. Discussion and conclusions

To make real impact on a clinical practice, engineers and scientists must be perfectly aware of the constraints of the clinic and the clinical workflow. In the context of aortic aneurysms, we need to consider carefully what data is actually available in a clinic and we should strive to obtain meaningful and clinically helpful results using only data available via standard-of-care diagnostic procedures as input to our computational biomechanics models. Non-invasive diagnostic methods that can identify patient-specific constitutive models of tissues and their parameters are not, and will not be for considerable time yet, available. Therefore, we advocate (as we have in the past, see e.g. Miller and Lu (2013) and Wittek et al. (2009)) modelling approaches which yield meaningful results that are weakly sensitive to the unknown tissue mechanical properties of a given patient.

The presented work is a step in this direction. We demonstrate an extremely simple modelling and simulation method of computing wall tension in abdominal aortic aneurysms. The inputs are just the (loaded) geometry of an aneurysm and blood pressure. No knowledge of the mechanical properties is needed. Moreover the computation itself is very simple and can be conducted on low cost and unobtrusive hardware in a clinic.

We have used fused CT and MRI datasets to estimate the aneurysm wall thickness at several points. The measured wall thicknesses were then interpolated to obtain an AAA with variable wall thickness, which allowed us to investigate the role of wall thickness on the computed stress fields. We postulate that substantial research effort needs to be invested into patient-specific AAA wall thickness measurement techniques, as only good estimates of the thickness yield good estimates of the stress.

We have shown that the proposed procedure can be also used for AAA models which include thrombus. Even with the inclusion of thrombus and variable wall thickness, the computed stress fields are only estimates of the real stress field, as there are still many simplifying assumptions and sources of errors which influence the results, such as: geometry (and especially thickness) can only be imperfectly approximated from medical images (due to the limited image accuracy), the arterial wall has multiple layers of various stiffness which are pre-stressed, the boundary conditions are not exactly known and the interaction with the surrounding organs is ignored. However one of the main conclusions of this contribution, that the geometry and loading might have more important effect on the results of biomechanical simulation than materials properties of tissues, is in agreement with a recent similar finding in the area of pelvic floor modelling (Mayeur et al. 2015).

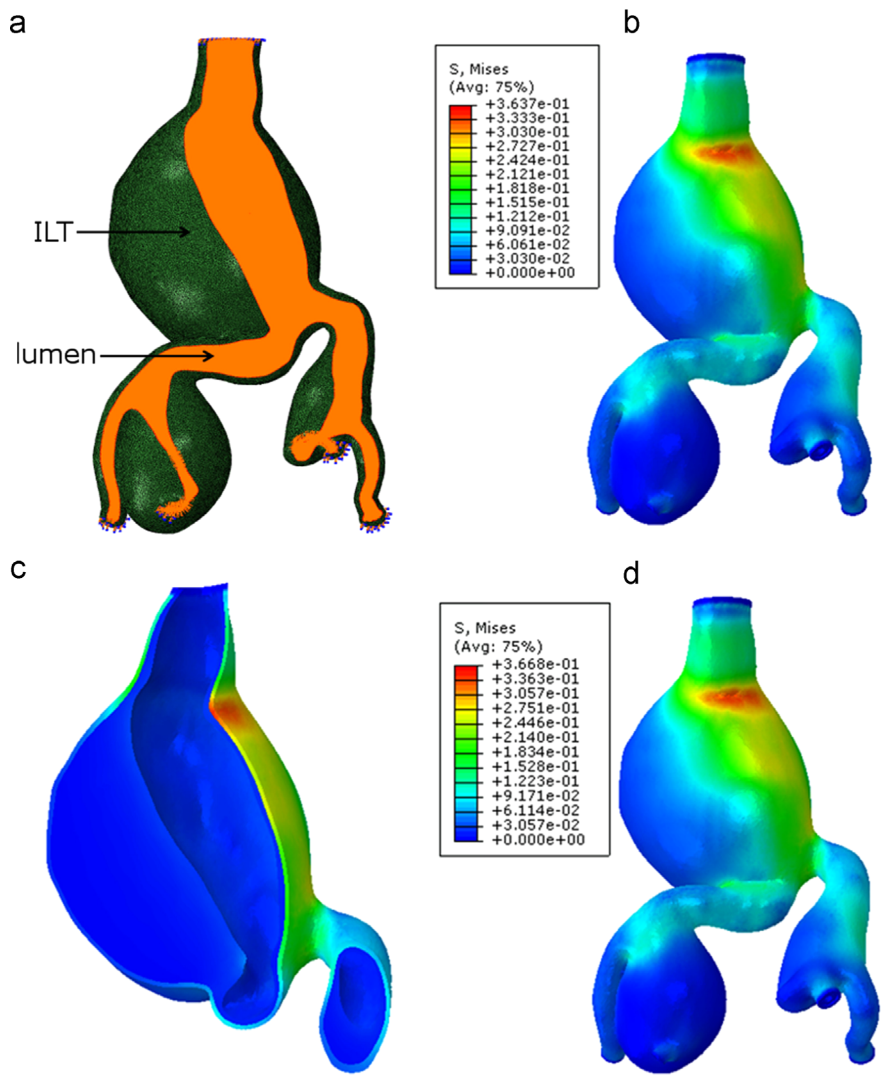

Fig. 11 – Analysis of a real AAA with thrombus under the assumption of constant wall thickness. (a) Geometry and boundary conditions, with uniform pressure loading to the luminal surface show in orange and proximal/distal ends constrained in all directions. The finite element mesh consists of approx. 675k tetrahedral elements and 148k nodes. (b) Computed stress field using nonlinear inverse procedure; $E_{wall}=2$ MPa, $E_{thrombus}=0.1$ MPa, max. von Mises stress = 0.364 MPa. (c) Stress field shown in a cut through the geometry of (b). The load creates much higher stress in the AAA wall than in the thrombus. (d) Stress distribution computed based on the deformed geometry and 10,000 stiffer materials; max. von Mises stress = 0.367 MPa (<1% difference).

Our approach of computing stresses is expected to work equally well for other approximately statically determinate structures in the human body, for which the loads and the deformed configuration can be measured, such as other types of aneurysms, the bowel and the bladder.

Acknowledgements

The financial support of the Australian Research Council (Discovery Grant no. DP120100402), the National Health and Medical Research Council (Grant nos. APP1063986 and APP1083572) and FNR Luxembourg Intermobility Programme is gratefully acknowledged. The authors would like to thank David Newby (The University of Edinburgh), Janet Powell (Imperial College London) and Paul Norman (The University of Western Australia) for providing the clinical cases used in this study.

REFERENCES

Budynas, R.G., Nisbett, J.K., Shigely, J.E., 2011. Shigley's Mechanical Engineering Design. McGraw-Hill, New York.

Di Martino, E.S., Bohra, A., Vande Geest, J.P., Gupta, N., Makaroun, M.S., Vorp, D.A., 2006. Biomechanical properties of ruptured versus electively repaired abdominal aortic aneurysm tissue. J. Vasc. Surg. 43, 570–576.

Doyle, B., Callanan, A., Mcgloughlin, T., 2007. A comparison of modelling techniques for computing wall stress in abdominal aortic aneurysms. Biomed. Eng. Online 6 (1), 38.

Doyle, B., Morris, L., Callanan, A., Kelly, P., Vorp, D., Mcgloughlin, T., 2008. 3D reconstruction and manufacture of real

abdominal aortic aneurysms: from CT scan to silicone model. J. Biomech. Eng. 130, 034501.
Doyle, B.J., Callanan, A., Grace, P.A., Kavanagh, E.G., 2013. On the influence of patient-specific material properties in computational simulations: a case study of a large ruptured abdominal aortic aneurysm. Int. J. Numer. Methods Biomed. Eng. 29 (2), 150–164.
Doyle, B.J., Cloonan, A.J., Walsh, M.T., Vorp, D.A., McGloughlin, T. M., 2010. Identification of rupture locations in patient-specific abdominal aortic aneurysms using experimental and computational techniques. J. Biomech. 43 (7), 1408–1416.
Doyle, B.J., Corbett, T.J., Cloonan, A.J., O'Donnell, M.R., Walsh, M. T., Vorp, D.A., Mcgloughlin, T.M., 2009. Experimental modelling of aortic aneurysms: novel applications of silicone rubbers. Med. Eng. Phys. 31 (8), 1002–1012.
Doyle, B.J., Killion, J., Callanan, A., 2012. Use of the photoelastic method and finite element analysis in the assessment of wall strain in abdominal aortic aneurysm models. J. Biomech. 45 (10), 1759–1768.
Doyle, B.J., McGloughlin, T.M., Miller, K., Powell, J.T., Norman, P.E., 2014. Regions of high wall stress can predict the future location of rupture of abdominal aortic aneurysm. Cardiovasc. Interv. Radiol. 37 (3), 815–818.
Erhart, P., Hyhlik-Durr, A., Geisbusch, P., Kotelis, D., Muller-Eschner, M., Gasser, T.C., Von Tengg-Kobligk, H., Bockler, D., 2015. Finite element analysis in asymptomatic, symptomatic, and ruptured abdominal aortic aneurysms: in search of new rupture risk predictors. Eur. J. Vasc. Endovasc. Surg. 49 (3), 239–245.
Gao, Y., Rathi, Y., Bouix, S., Tannenbaum, A., 2012. Filtering in the diffeomorphism group and the registration of point sets. IEEE Trans. Image Process. 21 (10), 4383–4396.
Gasser, T.C., Auer, M., Labruto, F., Swedenborg, J., Roy, J., 2010. Biomechanical rupture risk assessment of abdominal aortic aneurysms: model complexity versus predictability of finite element simulations. Eur. J. Vasc. Endovasc. Surg. 40 (2), 176–185.
Gasser, T.C., Nchimi, A., Swedenborg, J., Roy, J., Sakalihasan, N., Bockler, D., Hyhlik-Durr, A., 2014. A novel strategy to translate the biomechanical rupture risk of abdominal aortic aneurysms to their equivalent diameter risk: method and retrospective validation. Eur. J. Vasc. Endovasc. Surg. 47 (3), 288–295.
Gasser, T.C., Ogden, R.W., Holzapfel, G.A., 2006. Hyperelastic modelling of arterial layers with distributed collagen fibre orientations. J. R. Soc. Interface 3 (6), 15–35.
Hyhlik-Durr, A., Krieger, T., Geisbusch, P., Kotelis, D., Able, T., Bockler, D., 2011. Reproducibility of deriving parameters of AAA rupture risk from patient-specific 3D finite element models. J. Endovasc. Ther. 18 (3), 289–298.
IMPROVE Trial Investigators. 2014. Endovascular or open repair strategy for ruptured abdominal aortic aneurysm: 30 day outcomes from IMPROVE randomised trial. BMJ, 248:f7661.
Joldes, G.R., Wittek, A., Miller, K., 2015. A total lagrangian based method for recovering the un-deformed configuration in finite elasticity. Appl. Math. Model. 39 (14), 3913–3923, http://dx.doi.org/10.1016/j.apm.2014.12.013.
Li, Z.Y., Sadat, U., U-King-Im, J, Tang, T.Y., Bowden, D.J., Hayes, P.D., Gillard, J.H., 2010. Association between aneurysm shoulder stress and abdominal aortic aneurysm expansion: a longitudinal follow-up study. Circulation 122 (18), 1815–1822.
Lu, J., Zhou, X., Raghavan, M.L., 2007a. Computational method of inverse elastostatics for anisotropic hyperelastic solids. Int. J. Numer. Methods Eng. 69, 1239–1261.
Lu, J., Zhou, X., Raghavan, M.L., 2007b. Inverse elastostatic stress analysis in pre-deformed biological structures: demonstration using abdominal aortic aneurysms. J. Bimech. 40, 693–696.
Maier, A., Gee, M.W., Reeps, C., Pongratz, J., Eckstein, H.H., Wall, W.A., 2010. A comparison of diameter, wall stress, and rupture potential index for abdominal aortic aneurysm rupture risk prediction. Ann. Biomed. Eng. 38 (10), 3124–3134.
McBride, O.M.B., Berry, C., Burns, P., Chalmers, R.T.A., Doyle, B., Forsythe, R., Garden, O.J., Goodman, K., Graham, C., Hoskins, P., Holdsworth, R., Macgillivray, T.J., Mckillop, G., Murray, G., Oatey, K., Robson, J.M.J., Roditi, G., Semple, S., Stuart, W., Van Beek, E.J.R., Vesey, A., Newby, D.E., 2015. MRI using ultrasmall superparamagnetic particles of iron oxide in patients under surveillance for abdominal aortic aneurysms to predict rupture or surgical repair: MRI for abdominal aortic aneurysms to predict rupture or surgery—the MA3RS study. Open Heart 2, 1.
McGloughlin, T.M., Doyle, B.J., 2010. New approaches to abdominal aortic aneurysm rupture risk assessment: engineering insights with clinical gain. Arterioscler. Thromb. Vasc. Biol. 30 (9), 1687–1694.
Mayeur, O., Witz, J.F., Lecomte, P., Brieu, M.J., Cosson, M., Miller, K., 2015. Influence of geometry and mechanical properties on the accuracy of patient-specific simulation of women pelvic floor. Ann. Biomed. Eng. http://dx.doi.org/10.1007/s10439-015-1401-9.
Meyer, C.A., Bertrand, E., Boiron, O., Deplano, V., 2011. Stereoscopically observed deformations of a compliant abdominal aortic aneurysm model. J. Biomech. Eng. 133 (11), 111004.
Miller, K., Lu, J., 2013. On the prospect of patient-specific biomechanics without patient-specific properties of tissues. J. Mech. Behav. Biomed. Mater. 27, 154–166.
O'Leary, S., Kavanagh, E.G., Grace, P.A., McGloughlin, T.M., Doyle, B.J., 2014a. The biaxial mechancial behaviour of abdominal aortic aneurysm intraluminal thrombus: classification of morphology and the determination of layer and region specific properties. J. Biomech. 47, 1430–1437.
O'Leary, S.A., Healy, D.A., Kavanagh, E.G., Walsh, M.T., McGloughlin, T.M., Doyle, B.J., 2014b. The biaxial biomechancial behaviour of abdominal aortic aneurysm tissue. Ann. Biomed. Eng. 42, 2440–2450.
Raghavan, M., Vorp, D., Federle, M., Makaroun, M., Webster, M., 2000. Wall stress distribution on three-dimensionally reconstructed models of human abdominal aortic aneurysm. J. Vasc. Surg. 31, 760–769.
Riveros, F., Chandra, S., Finol, E.A., Gasser, T.C., Rodriguez, J.F., 2013. A pull-back algorithm to determine the unloaded vascular geometry in anisotropic hyperelastic AAA passive mechanics. Ann. Biomed. Eng. 41 (4), 694–708.
Shang, E.K., Lai, E., Pouch, A.M., Hinmon, R., Gorman, R.C., Gorman III, J.H., Sehgal, C.M., Ferrari, G., Bavaria, J.E., Jackson, B.M., 2015. Validation of semiautomated and locally resolved aortic wall thickness measurements from computed tomography. J. Vasc. Surg. 61 (4), 1034–1040.
Tong, J., Cohnert, T., Regitnig, P., Holzapfel, G.A., 2011. Effects of age on the elstic properties of the intraluminal thrombus and the thrombus-covered wall in abdominal aortic aneurysms: biaxial extensino behaviour and material modelling. Eur. J. Vasc. Endovasc. Surg. 42, 207–219.
Vande Geest, J., Wang, D., Wisniewski, S., Makaroun, M., Vorp, D., 2006a. Towards a non-invasive method for determination of patient-specific wall strength distribution in abdominal aortic aneurysms. Ann. Biomed. Eng. 34 (7), 1098–1106.
Vande Geest, J.P., Di Martino, E.S., Bohra, A., Makaroun, M.S., Vorp, D.A., 2006b. A biomechanics-based rupture potential index for abdominal aortic aneurysm risk assessment: demonstrative application. Ann. N. Y. Acad. Sci. 1085, 11–21.
Vande Geest, J.P., Sacks, M.S., Vorp, D.A., 2006c. The effects of aneurysm on the biaxial mechancial behaviour of human abdominal aorta. J. Biomech. 39, 1324–1334.
Wittek, A., Hawkins, T., Miller, K., 2009. On the unimportance of constitutive models in computing brain deformation for image-guided surgery. Biomech. Model. Mechanobiol. 8 (1), 77–84.